High-P tectono-metamorphic evolution of mylonites from the Variscan basement of the Northern Apennines, Italy

High-*P* tectono-metamorphic evolution of mylonites from the Variscan basement of the Northern Apennines, Italy

Deborah Lo Pò[1] | Roberto Braga[1] | Hans-Joachim Massonne[2] | Giancarlo Molli[3] | Alessandra Montanini[4] | Giuseppe M. Bargossi[1]

[1]Dipartimento di Scienze Biologiche, Geologiche e Ambientali, Università di Bologna, Bologna,Italy

[2]Institut fur Mineralogie und Kristallchemie, Universitat Stuttgart, Stuttgart,Germany

[3]Dipartimento di Scienze della Terra, Università di Pisa, Pisa,Italy

[4]Dipartimento di Scienze Chimiche, della Vita e della Sostenibilità Ambientale, Università di Parma, Parma, Italy

Correspondence
Deborah Lo Pò, Dipartimento di Scienze Biologiche, Geologiche e Ambientali, Università di Bologna, Bologna, Italy.
Email: deborah.lopo@unibo.it

Funding information
University of Bologna

Handling Editor: Doug Robinson

Abstract

Strain localization within shear zones may partially erase the rock fabric and the metamorphic assemblage(s) that had developed before the mylonitic event. In poly-deformed basements, the loss of information on pre-kinematic phases of mylonites hinders large-scale correlations based on tectono-metamorphic data. In this study, devoted to a relict unit of Variscan basement reworked within the nappe stack of the Northern Apennines (Italy), we investigate the possibility to reconstruct a complete pressure (*P*)–temperature (*T*)–deformation (*D*) path of mylonitic micaschist and amphibolite by integrating microstructural analysis, mineral chemistry and thermodynamic modelling. The micaschist is characterized by a mylonitic fabric with fine-grained K-white mica and chlorite enveloping mica-fishes, quartz, and garnet pseudomorphs. Potassic white mica shows Mg-rich cores and Mg-poor rims. The amphibolite contains green amphibole+plagioclase+garnet+quartz+ilmenite defining S_1 with a superposed mylonitic fabric localized in decimetre- to centimetre-scale shear zones. Garnet is surrounded by an amphibole+plagioclase corona. Phase diagram calculations provide *P–T* constraints that are linked to the reconstructed metamorphic-deformational stages. For the first time an early high-*P* stage at >11 kbar and 510°C was constrained, followed by a temperature peak at 550–590°C and 9–10 kbar and a retrograde stage (<475°C, <7 kbar), during which ductile shear zones developed. The inferred clockwise *P–T–D* path was most likely related to crustal thickening by continent-continent collision during the Variscan orogeny. A comparison of this *P–T–D* path with those of other Variscan basement occurrences in the Northern Apennines revealed significant differences. Conversely, a correlation between the tectono-metamorphic evolution of the Variscan basement at Cerreto pass, NE Sardinia and Ligurian Alps was established.

KEYWORDS
High *P* metamorphism, mylonite, Northern Apennines, *P T D* path, Variscan orogeny

1 | INTRODUCTION

The effects of high-strain and re-equilibration occurring in shear zones may obliterate most of the pre-existing minerals and structures in mylonitic rocks. Therefore, the early evolution of such rocks is usually tricky to unravel and this difficulty hampers the reconstruction of a complete metamorphic history. However, a *P–T* path involving early

stages of the metamorphic evolution is essential, for instance, to establish correlations among basement units and to reconstruct geodynamic scenarios. The application of thermodynamic modelling, coupled with microstructural observations and mineral composition analyses, to mylonitized rocks was tested here in order to assess if this methodological approach can establish a complete *P–T–D* path, including the pre-mylonitic stages.

The study was carried out on mylonitic medium-grade metapelites and associated amphibolites from the Cerreto pass, belonging to the Variscan basement of the Northern Apennines, a remnant of a southern portion of the Variscan belt (e.g., Franceschelli, Gianelli, Pandeli, & Puxeddu, 2004; Lo Pò & Braga, 2014; Lo Pò, Braga, & Massonne, 2016; Lo Pò, Braga, Massonne, Molli, et al., 2016; Molli, Montanini, & Frank, 2002). To date, only classical geothermobarometry has been used to decipher the metamorphic evolution of these rocks which suffered severe retrogression and shearing (Molli et al., 2002). A combined microstructural–petrological study, including phase diagram calculations, provides new *P–T* constraints for the recognized metamorphic–deformational phases. These calculations result in an improved *P–T–D* path for the Cerreto basement. This path elucidates diverse aspects of the Variscan metamorphism in the Northern Apennines, for instance the occurrence of a high-*P* event. The obtained evolution for the Cerreto basement is compared with the thermobaric history of coeval south-European Variscan units outcropping in the neighborhood in order to establish possible correlations.

2 | GEOLOGICAL FRAMEWORK

The studied samples belong to the Variscan basement of the Northern Apennines (Franceschelli et al., 2004; Ricci, 1968; Vai, 2003), a remnant of Variscan chain in Italy (Figure 1a). The Northern Apennines is a nappe-pile edifice formed after the collision of the European (the Sardinia–Corsica block) and African (the Adria microplate) margins in Oligocene times (Vai & Martini, 2001). This edifice consists of oceanic and continental units (from top to the bottom):

1. Ligurian units: ophiolites derived from the oceanic lithosphere of the Western Tethys and their Mesozoic–Cenozoic sedimentary cover (Elter, 1975).
2. Tuscan Nappe and external foreland units: a continental Triassic–Tertiary sedimentary sequence detached from its original basement and unaffected by Alpine metamorphism (Bernoulli, 2001; Molli, 2008).
3. Tuscan Metamorphic units: Variscan basement and its Triassic–Oligocene cover, belonging to the Adria-derived continental sequence, both metamorphosed during the Alpine orogenic cycle (Franceschelli et al., 2004).

The Variscan basement of the Northern Apennines (Conti, Di Pisa, Gattiglio, & Meccheri, 1993; Franceschelli et al., 2004; Lo Pò & Braga, 2014; Lo Pò, Braga, & Massonne, 2016; Lo Pò, Braga, Massonne, Molli, et al., 2016) consists of low- to medium-grade metamorphic rocks. It is exposed in the study area at the Cerreto pass, in the Tuscan metamorphic ridge (Punta Bianca, Alpi Apuane, Monti Pisani, Monticiano-Monti Leoni), and on the Elba island. In addition, drilling has detected this basement in the subsurface of Pontremoli and Larderello (Figure 1b). The Variscan basement in the Larderello subsurface has been subdivided into three tectonic units (Batini, Brogi, Lazzarotto, Liotta, & Pandeli, 2003; Bertini, Casini, Gianelli, & Pandeli, 2006):

1. Phyllitic–quartzitic complex: low-grade metasedimentary rocks and metabasite layers, overprinted by the Alpine metamorphism and correlated with the Variscan succession from the Apuane Alps, Monti Pisani and Punta Bianca.
2. Micaschist complex: two-mica garnet-bearing albite micaschists with minor amphibolites, which were derived from ocean-floor basalts (OFB), affected by polymetamorphism during the Variscan and Alpine orogeneses.
3. Gneiss complex: muscovite–biotite paragneisses with orthogneiss, OFB amphibolite layers and calc-silicate rocks, affected only by Variscan metamorphism.

The Cerreto metamorphic rocks represent the northernmost occurrence of the Variscan basement in the Apennines, and are usually correlated with the micaschist complex of the Larderello subsurface (Pandeli, Gianelli, & Morelli, 2005). They consist of mylonitic micaschists with minor bodies of amphibolites exposed over an area of ~80 hm^2. The mylonitic fabric is more strongly developed within the micaschists than in the associated amphibolites. The whole micaschist–amphibolite complex occurs as a tectonic slice enclosed in very low grade Triassic quartzite within Late Triassic evaporites and dolomites (Anidriti di Burano Formation). The contact between micaschists and amphibolites is commonly covered by debris. The main foliation in the amphibolites was dated at 328–312 Ma by Ar–Ar on hornblende separates (Molli et al., 2002) confirming that the Cerreto metamorphic rocks were involved in the collisional stage of the South-European Variscides. This amphibolite stage (650°C, 8 kbar) was followed by a retrograde mylonitic stage at 530°C and 4–5 kbar (Molli et al., 2002). In this study, we investigated a micaschist (PC1) and an amphibolite (CER4) from the Cerreto pass and performed

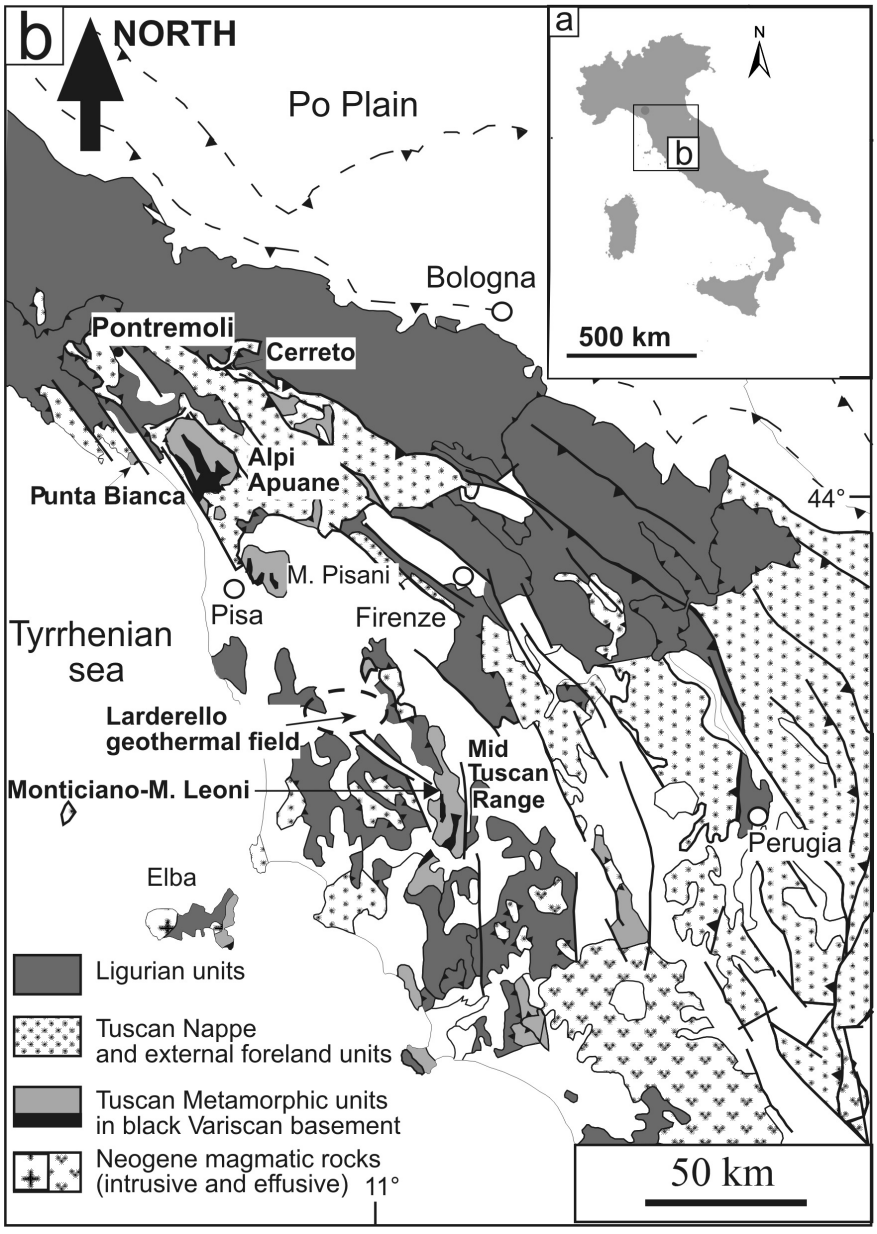

FIGURE 1 Location of the Northern Apennines in Italy (a) and regional geological framework of the Northern Apennines with the distribution of the Variscan basement in black (b; modified after Lo Pò, Braga, Massonne, Molli, et al., 2016)

thermodynamic modelling on these rocks. PC1 and CER4 crop out at 44°18′28″N, 10°11′52″E and 44°18′30″N, 10°11′56″E, respectively.

3 | ANALYTICAL METHODS

Petrographic observations and microstructural analyses were performed with a polarising optical microscope and a scanning electron microscope Philips 515B at the Dipartimento di Scienze Biologiche, Geologiche ed Ambientali (Università di Bologna). The chemical composition of the minerals in the micaschist PC1 was acquired using a CAMECA SX100 electron microprobe (EMP) equipped with five wavelength dispersive (WD) spectrometers at the Institut für Mineralogie und Kristallchemie (Universität Stuttgart). Na, Mg, Al, Si, K, Ca, Ti, Mn, Fe, Ba, Cr were analysed in white mica, chlorite and plagioclase with an acceleration voltage of 15 kV and a beam current of 10–15 nA. Counting times for each element were 20 s at the peak and the background. Synthetic and natural minerals and pure oxides were used as standards. The raw data were corrected using the PaP correction procedure. The errors of the applied method are given by Massonne (2012). X-ray maps (Fe, Mg, Ti, Na) of white mica were prepared using a counting time of 100 ms, a step width of 1 μm, an acceleration voltage of 15 kV and a current of 30 nA. Structural formulae for white mica, chlorite and plagioclase were calculated with the CalcMin program (Brandelik, 2009). X-ray maps were elaborated with the XMap software

(Bernhardt, Massonne, Reinecke, Reinhardt, & Willner, 1995, and updates).

The bulk-rock composition of micaschist PC1 was determined through WD-XRF analysis on a pressed powder pellet using a Philips PW1480 and an Axios-Panalytical spectrometer at the Dipartimento di Scienze Biologiche, Geologiche e Ambientali, Università di Bologna. The sample preparation and the instrumental set-up were reported by Braga and Cinelli (2014). Loss on ignition was obtained with standard gravimetric procedures, after heating the powder at 950°C for 12 hr. The mineral and rock-chemistry of CER4 were taken from Molli et al. (2002).

4 | PETROGRAPHY AND MICROSTRUCTURAL ANALYSIS

4.1 | Micaschists

The mylonitic micaschists contain pre-kinematic microstructures (Figure 2a,b) and a shearing fabric (Figure 2c,d). Shear bands and mantled porphyroclasts commonly indicate a dextral sense of shear (i.e. top to the NE in present day setting). Only few samples contain garnet porphyroclasts whereas most exhibit garnet pseudomorphed by chlorite (Figure 2e). Muscovite–paragonite–chlorite intergrowths occur at the μm scale (Figure 2f). Ultramylonitic levels occasionally cut the mylonitic foliation. Accessory minerals are pyrite, epidote, K-feldspar and titanite.

PC1 is a mylonitic micaschist showing garnet pseudomorphs, quartz porphyroclasts and mica-fish (some hundreds of μm long), mantled by a fine-grained (few tens of μm thick) white mica-chlorite mylonitic foliation. The quartz porphyroclasts (some hundreds of μm in diameter) host chlorite and white mica inclusions. Large quartz crystals are surrounded by quartz subgrains with sutured grain boundaries. The recrystallized quartz shows an oblique shape preferred orientation in some domains. The mylonitic foliation is locally crenulated (Figure 2c), or associated with C′-type shear bands. Asymmetric foliation boudins consisting of white mica aggregates are also present. Garnet is totally pseudomorphosed by chlorite (Figure 2e). The modal content of these pseudomorphs is 3 vol.%, determined through image analysis of a thin-section photograph with the JMicroVision 1.2.7 software (http://www.jmicrovision.com/). Feldspar is locally found in the mylonitic foliation. Ilmenite, rutile, titanite, allanite, epidote, pyrite, tourmaline, apatite and zircon are accessory minerals. Ilmenite is xenoblastic and forms fish-shaped crystals and boudins. It contains inclusions of rutile and biotite (Figure 2b). Titanite is oriented parallel to the mylonitic foliation and may form irregular rims around ilmenite (Figure 2b). Epidote has allanite cores.

Based on the occurrence of coarse-grained K-white mica, rutile and biotite inclusions in ilmenite, chlorite inclusions in quartz porphyroclasts, garnet porphyroclasts and ilmenite-fishes, the assemblage K-white mica+biotite+chlorite+quartz+garnet+rutile+ilmenite in PC1 is attributed to a metamorphic event (M_1) predating mylonitization (Figure 2a,b,d,e). Fine-grained K-white mica+chlorite+quartz+plagioclase+titanite are oriented along the mylonitic foliation. These minerals hence formed by shearing during the syn-kinematic event (M_2). The same event is also responsible for the development of an oblique foliation in quartz, C′-shear bands, asymmetric foliation boudins and the deformation of pre-kinematic minerals (mica and ilmenite fishes, quartz, garnet and plagioclase porphyroclasts) in the micaschist (Figure 2a–e). Titanite surrounding ilmenite and chlorite replacing garnet also formed during M_2.

4.2 | Amphibolites

The amphibolites associated with the micaschists are foliated, fine-grained rocks showing a schistosity (S_1), which is locally crosscut by millimetre- to decimetre-wide mylonitic to ultramylonitic shear zones (Figure 2g).

CER4 contains green amphibole+plagioclase+garnet+quartz+ilmenite+chlorite defining S_1 (M_1). Apatite is an accessory mineral. Garnet occurs as rounded pre-kinematic porphyroclasts with a diameter up to 5 mm. It typically shows an amphibole+plagioclase corona (Figure 2h), and can be partially or totally replaced by chlorite, quartz, amphibole, plagioclase, epidote and titanite (M_2).

5 | ROCK AND MINERAL COMPOSITION

5.1 | PC1

The bulk-rock composition (Table 1) is similar to Post-Archean Australian Shale (Taylor & McLennan, 1985) and

FIGURE 2 Petrographic features of the Cerreto metamorphic rocks (a f refer to micaschists, g and h to amphibolites): (a) external foliation (S_e) surrounding a plagioclase porphyroclast, which exhibits an internal foliation (S_i) (CER7; crossed nicols microphotograph from Molli et al., 2002); (b) rutile in an ilmenite grain surrounded by titanite (PC1; BSE image); (c) folded mylonitic foliation (PC1; BSE image); (d) mica and ilmenite fish (PC1; BSE image); (e) fractured and retrogressed garnet porphyroclast (PC1; plane polarized light microphotograph); (f) K white mica+Na white mica+ chlorite intergrowths forming an asymmetric foliation boudin (PC23; BSE image); (g) matrix in amphibolite crosscut by a mylonitic foliation (CER6; plane polarized light microphotograph from Molli et al., 2002); (h) garnet porphyroclast surrounded by an amphibole+plagioclase corona (CER4; crossed nicols microphotograph)

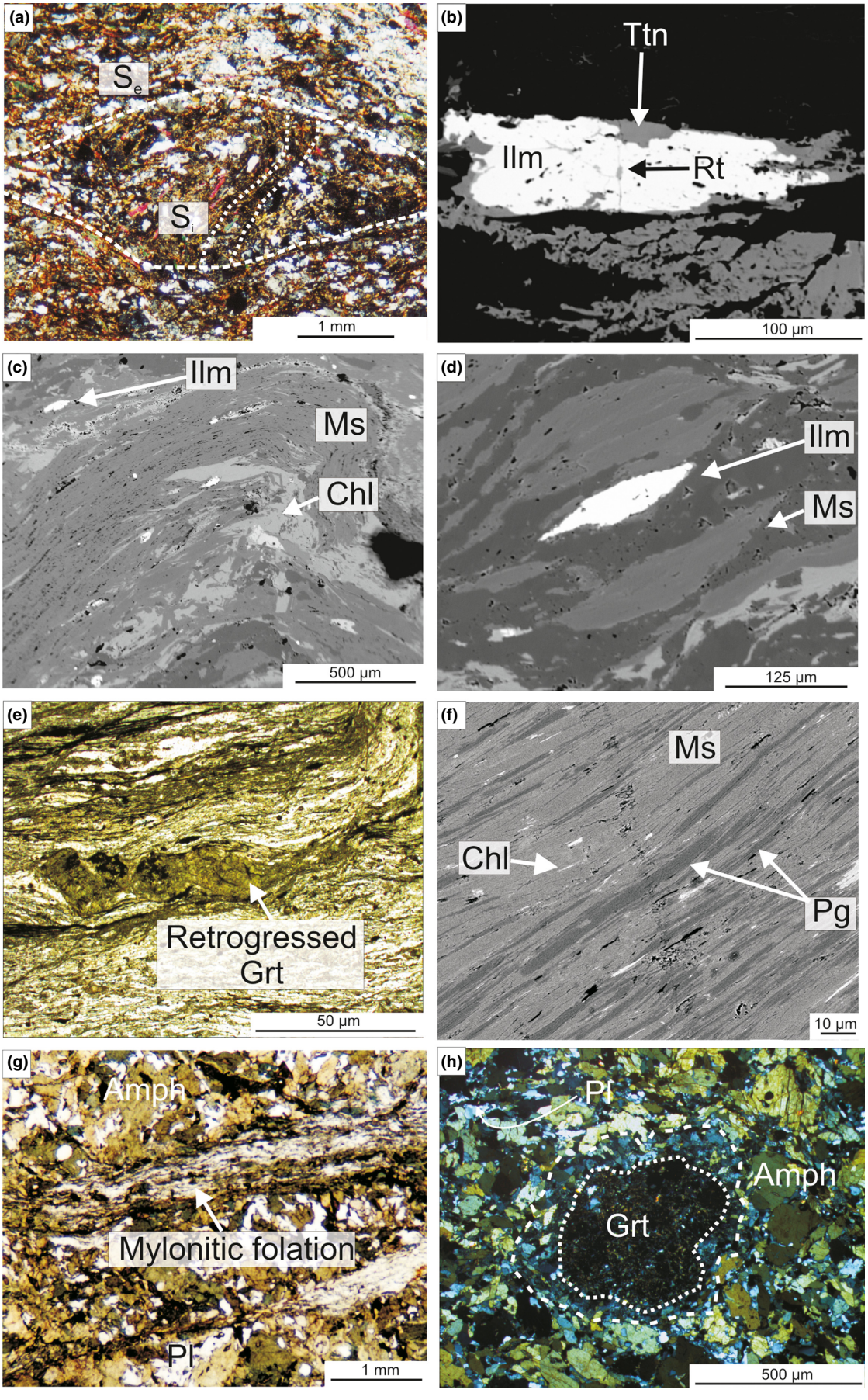
(a)
S_e
S_i
1 mm
(b)
Ttn
Ilm
Rt
100 µm
(c)
Ilm
Ms
Chl
500 µm
(d)
Ilm
Ms
125 µm
(e)
Retrogressed Grt
50 µm
(f)
Ms
Chl
Pg
10 µm
(g)
Amph
Mylonitic folation
Pl
1 mm
(h)
Pl
Amph
Grt
500 µm

TABLE 1 Bulk rock composition of PC1 determined through WD XRF analysis (this work), (unfractionated) CER4 from Molli et al. (2002) and CER4 after garnet fractionation (calculated in this study). Compositions modified for thermodynamic modelling (see text) are also presented

	XRF (wt%)			Thermodynamic modelling (wt%)		
		CER4			CER4	
	PC1	Unfractionated	Fractionated	PC1	Unfractionated	Fractionated
SiO_2	67.74	49.49	49.68	70.53	50.99	51.68
TiO_2	0.85	2.5	2.58	0.89	2.58	2.68
Al_2O_3	16.9	12.18	11.67	17.6	12.55	12.14
Fe_2O_3	4.61	17.22	16.58			
FeO				4.32	15.95	15.51
MnO	0.05	0.27	0.00	0.06	0.28	
MgO	1.53	6.01	6.18	1.59	6.19	6.43
CaO	0.75	9.44	9.38	0.53	9.20	9.21
Na_2O	1.59	2.19	2.27	1.66	2.26	2.36
K_2O	2.71	0.31	0.32	2.83		
P_2O_5	0.18	0.39	0.40			
L.O.I.	3.08	0.94	0.94			
H_2O				In excess	In excess	In excess
Total	99.99	100.94	100.00	100	100	100

L.O.I., loss on ignition.

Upper Continental Crust (McLennan, 2001), except for CaO, which is depleted in PC1 with respect to these mean rock compositions. In the Fe_2O_3/K_2O *v.* SiO_2/Al_2O_3 diagram (Herron, 1988; not shown), PC1 plots at the wacke-shale boundary.

Pre-kinematic white mica (Ms_1) is potassic and characterized by Mg-rich cores and Mg-poor rims as evident from X-ray mapping (Figure 3a,b). The Mg-rich pre-kinematic K-white mica has Si = 3.17–3.30 atoms per formula unit (apfu), Mg = 0.14–0.22 apfu and Na = 0.04–0.06 apfu. The Mg-poor pre-kinematic K-white mica has Si = 3.03–3.08 apfu, Mg = 0.05–0.08 apfu, Na = 0.15–0.27 apfu. Potassic white mica oriented along the mylonitic foliation (Ms_2) also shows a variable composition with Si = 3.06–3.19 apfu, Mg = 0.06–0.23 apfu, Na = 0.02–0.10 apfu (Figure 4a–c; Table 2). Chlorite from the mylonitic foliation has Si = 5.15–5.93 apfu, Al^{IV} = 2.07–2.85 apfu, Al^{VI} = 2.21–3.34 apfu and X_{Fe}=Fe/(Fe+Mg) = 0.50–0.60

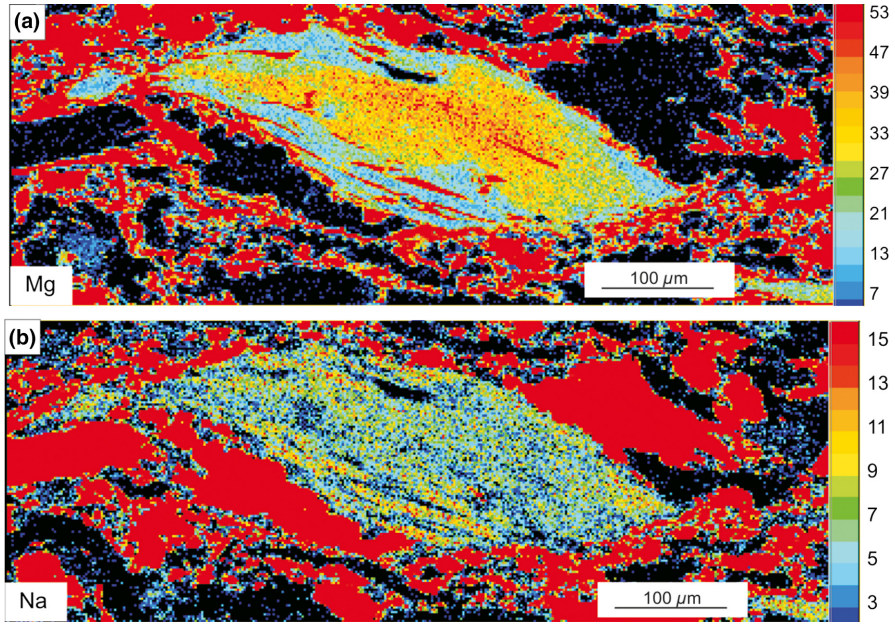

FIGURE 3 X ray maps of K white mica in PC1 (a) Mg distribution; (b) Na distribution. The colour code scales are related to the counts of specific Kα radiation per time unit

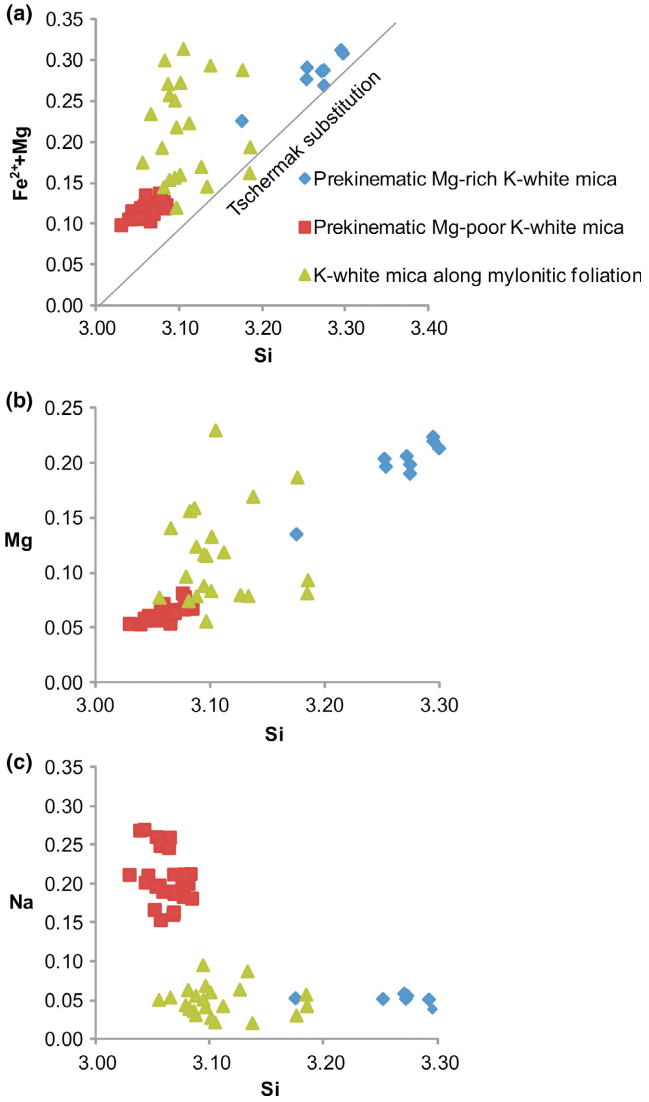

FIGURE 4 Compositional diagrams for K white mica in PC1: (a) Fe^{2+}+Mg *v.* Si; (b) Mg *v.* Si; (c) Na *v.* Si. Additional analyses not reported in Table 2 are also shown

(Table 3). Feldspar along the mylonitic foliation is albite ($Ab_{94-99}An_{0-5}Or_{0-4}$) with K-feldspar ($Ab_{0-1}An_{2-5}Or_{95-97}$) exsolutions (Table 3).

5.2 | CER4

Mineral and bulk compositions of the amphibolite (CER4) are from Molli et al. (2002). The protolith of CER4 was a mafic igneous rock (Molli et al., 2002), according to the projection of bulk-rock major element composition in the (Al+Fe+Ti) *v.* (Ca+Mg) diagram of Moine and De La Roche (1968; not shown in Molli et al., 2002; and in this study). We calculated the effective bulk-composition after fractionation of some elements into garnet (Table 1), since zoned minerals are removed from the reacting rock volume during cooling (Stüwe, 1997). The average garnet composition was subtracted from the XRF bulk composition, following the approach of Lo Pò, Braga, Massonne, Molli, et al. (2016). For this purpose, the densities of the rock (3.1 g/cm^3) and of garnet (4.1 g/cm^3) were calculated with PERPLE X (see below) at *P–T* conditions at which the garnet rim formed (see "Section 6.3"). The modal content of garnet (3 vol.%) was determined with the JMicroVision 1.2.7 software (see above). The resulting fractionated bulk composition is depleted in Al_2O_3, FeO and enriched in SiO_2, TiO_2, MgO, CaO, Na_2O relative to the unfractionated bulk-rock composition (Table 1). Manganese is totally sequestered in garnet.

The amphibole classification follows the IMA nomenclature (Leake et al., 2004). Amphibole occurring along S_1 ($Amph_1$) and replacing garnet ($Amph_2$) is unzoned ferrotschermakite. Si and Al^{IV} in $Amph_1$ range from 6.28 to 6.30 apfu and from 1.70 to 1.72 apfu, respectively. $Amph_2$ has Si = 5.98–6.18 apfu and Al^{IV} = 1.82–2.02 apfu. Plagioclase along S_1 (Pl_1) is oligoclase ($Ab_{80}An_{20}$). Plagioclase in garnet pseudomorphs (Pl_2) is oligoclase–andesine ($Ab_{64-80}An_{20-36}$). Garnet is almandine-rich showing an increase in Fe and a decrease in Mn from core ($Alm_{54}Grs_{23}Sps_{16}Prp_4Adr_4$) to rim ($Alm_{58}Grs_{23}Sps_{11}Prp_5Adr_3$).

6 | GEOTHERMOBAROMETRY

6.1 | Isochemical phase diagram calculations

Isochemical phase diagrams (pseudosections) were calculated for micaschist PC1 and amphibolite CER4 with the PERPLE X program package (Connolly, 1990; Connolly & Petrini, 2002). The considered *P–T* range is 350–600°C and 2–15 kbar. Silica (only for PC1) and H_2O were considered to be in excess. The pseudosection for micaschist PC1 was calculated in the MnCKNFMASHT system assuming all iron to be totally ferrous because no Fe^{3+}-oxides are present and minerals with significant Fe^{3+} amounts (i.e. epidote) occur in low quantities (<1 vol.%). The bulk-rock composition was recalculated discarding P_2O_5 and reducing the CaO content by the amount bound to apatite (Table 1). The thermodynamic data set of Holland and Powell (1998, with the 2002 upgrade), the compensated Redlich Kwong (CORK) fluid equation of state by Holland and Powell (1991, 1998), and the following solid-solution models were used: Pheng(HP) for K-white mica (Holland & Powell, 1998; the maximum paragonite content set to 50 mol.%), Mica(M) for Na–Ca white mica (Massonne, 2010; the maximum muscovite content was set to 50 mol.%), Gt(HP) for garnet (Holland & Powell, 1998), TiBio(HP) for biotite (Powell & Holland, 1999; White, Powell, Holland, & Worley, 2000), Chl(HP) for chlorite (Holland, Baker, & Powell, 1998), feldspar for plagioclase (Fuhrman & Lindsley, 1988), St(HP) for staurolite (Holland & Powell, 1998), and the ideal models (see http://www.perplex.ethz.ch/Perple

TABLE 2 Representative mineral compositions of K white mica in micaschist PC1. The formula of K white mica is calculated assuming 42 (Ca+Ba) valencies and 4 H

K-white mica									
	Prekinematic Mg-rich core			Prekinematic Mg-poor rim			Mylonitic foliation		
Point analyses	Ms11 4	Ms11 5	Ms11 6	Ms08 1	Ms9 2	Ms9 3	Ms10 01	Ms10 02	Ms10 03
SiO_2	50.13	49.69	50.62	46.40	47.05	46.38	46.39	45.55	45.10
TiO_2	0.30	0.33	0.38	0.14	0.46	0.40	0.37	0.36	0.31
Al_2O_3	31.45	31.33	30.95	34.78	35.45	36.15	33.85	34.50	34.12
FeO	1.64	1.43	1.66	2.15	1.09	0.98	1.87	1.33	1.69
MnO	0.05						0.04		
MgO	2.04	1.94	2.30	1.10	0.87	0.72	1.19	0.78	0.95
CaO	0.04	0.03	0.01		0.03	0.01	0.02	0.01	0.01
Na_2O	0.42	0.39	0.39	0.35	0.92	0.91	0.33	0.43	0.33
K_2O	10.56	10.76	10.46	10.94	10.56	10.35	10.65	10.93	10.60
BaO	0.19	0.20	0.15	0.35	0.24	0.27	0.34	0.25	0.32
Total	96.82	96.11	96.91	96.20	96.67	96.18	95.04	94.13	93.44
Si	3.27	3.27	3.29	3.09	3.09	3.06	3.11	3.09	3.08
Al^{IV}	0.73	0.73	0.71	0.91	0.91	0.94	0.89	0.91	0.92
Ti	0.01	0.02	0.02	0.01	0.02	0.02	0.02	0.02	0.02
Al^{VI}	1.70	1.71	1.67	1.81	1.84	1.87	1.79	1.84	1.82
Fe^{2+}	0.09	0.08	0.09	0.12	0.06	0.05	0.10	0.08	0.10
Mn	0.00						0.00		
Mg	0.20	0.19	0.22	0.11	0.09	0.07	0.12	0.08	0.10
Ca	0.00	0.00	0.00		0.00	0.00	0.00	0.00	0.00
Na	0.05	0.05	0.05	0.04	0.12	0.12	0.04	0.06	0.04
K	0.88	0.90	0.87	0.93	0.89	0.87	0.91	0.95	0.92
Ba	0.00	0.01	0.00	0.01	0.01	0.01	0.01	0.01	0.01

X solution model glossary.html) hCrd for cordierite and IlGkPy for ilmenite. Pure phases are, for instance, titanite, rutile, zoisite, lawsonite, sillimanite and andalusite.

For the thermodynamic modelling of the amphibolite CER4, the XRF composition given by Molli et al. (2002) was used, converting $Fe_2O_3{}^{tot}$ to FeO^{tot}, reducing CaO according to P_2O_5 in apatite (see above) and eliminating K_2O because of its negligible concentration (Table 1). Two *P–T* pseudosections were calculated, in the MnCNFMASHT and CNFMASHT systems in order to determine the M_1 and M_2 conditions, respectively. The latter was calculated using the fractionated bulk-rock composition in a Mn-free system due to the sequestration of the bulk Mn into garnet. For the calculations based on the amphibolites CER4, the solid-solution models GlTrTsPg (Powell & Holland, 1999) and Act (M) (Massonne & Willner, 2008) for amphibole and Omph (HP) for clinopyroxene (Holland & Powell, 1996) were additionally considered.

The obtained pseudosections were contoured by isopleths for Si in K-white mica and modal amount of garnet (micaschist) and molar fractions of garnet components and anorthite in plagioclase (amphibolite).

6.2 | Modelling results for micaschist PC1

In the pseudosection for micaschist PC1 (Figure 5), K-white mica is present over the entire *P–T* grid. The Na–Ca white mica disappears above 520°C at 2 kbar and below 5 kbar at 600°C. Chlorite breaks down above 520°C, 2 kbar and 580°C, 15 kbar. Biotite appears at 450°C, 8 kbar. Garnet occurs above 400°C, >11 kbar. Plagioclase is present below 7 kbar and above 380°C. Rutile disappears below 9 kbar above 525°C. Ilmenite coexists with rutile at 450°C, 2 kbar to 500°C, 9 kbar. Ilmenite replaces rutile above 550°C below 10 kbar completely. The titanite-out curve is at 380°C, 2 kbar and 500°C, 12 kbar. The Si in K-white mica increases with pressure reaching a maximal 3.39 apfu. The isopleth for the maximum measured Si of the Mg-rich pre--kinematic K-white mica (3.30 apfu) plots at pressures above 10 kbar. An early stage of M_1 (prograde stage) can be

TABLE 3 Representative mineral compositions of chlorite and feldspar in micaschist PC1. The structural formula of chlorite is calculated on the basis of 28 oxygen and 16 H, neglecting Na and Ca. The structural formula of plagioclase is based on 8 oxygen

	Chlorite				Feldspar				
	Mylonitic foliation				Mylonitic foliation			Exsolution in plagioclase	
Point analyses	Chl06 02	Chl06 03	Chl06 04	Chl06 05	Pl01	Pl06 10	Pl03	Kfs03	Kfs04
SiO_2	24.20	24.41	23.93	25.67	68.03	68.27	67.94	64.39	65.00
TiO_2	0.06	0.06	0.07	0.07	0.07	0.00	0.10	0.00	0.00
Al_2O_3	22.05	22.06	22.07	21.85	20.71	20.05	20.97	18.52	18.30
FeO^{tot}	28.85	28.88	28.87	28.49					
Fe_2O_3					0.45	0.09	0.31	0.27	0.28
MnO	0.21	0.23	0.23	0.26					
MgO	12.55	12.89	12.52	12.20	0.00	0.00	0.03	0.00	0.01
CaO					0.84	0.67	1.11	0.02	0.00
Na_2O					11.67	11.59	11.55	0.54	0.31
K_2O					0.10	0.07	0.11	16.54	16.39
BaO					0.00	0.00	0.00	0.33	0.17
Total	87.91	88.53	87.69	88.54	101.88	100.73	102.12	100.61	100.45
Si	5.19	5.20	5.15	5.43	2.93	2.97	2.92	2.98	3.00
Ti	0.01	0.01	0.01	0.01	0.00	0.00	0.00	0.00	0.00
Al	5.58	5.54	5.60	5.45	1.05	1.03	1.06	1.01	0.99
Fe^{3+}					0.01	0.00	0.01	0.01	0.01
Fe^{tot}	5.18	5.14	5.20	5.04					
Mn	0.04	0.04	0.04	0.05					
Mg	4.02	4.09	4.02	3.85					
Ca					0.04	0.03	0.05	0.00	
Na					0.98	0.98	0.96	0.05	0.03
K					0.01	0.00	0.01	0.98	0.96
Ba									
X_{An}					0.04	0.03	0.05	0.01	0.00
X_{Ab}					0.96	0.97	0.94	0.05	0.03
X_{Or}					0.01	0.00	0.01	0.95	0.97

constrained above 11 kbar and 510°C by the intersection of this isopleth and the *P–T* boundaries of biotite-bearing, titanite-absent assemblage fields.

The calculated paragenesis, corresponding to the inferred M_1 mineral assemblage (Ms+Chl+Bt+Grt+Il+Rt+Qtz) except for paragonite, plots at 520–590°C and 9–10 kbar. The estimated garnet modal quantity (3 vol.%) plots above 500°C and 8 kbar. The corresponding isomode occurs in the M_1 mineral assemblage field at 550–590°C and 9–10 kbar, defining the peak stage of the M_1 event.

The *P–T* conditions of the M_2 event were determined considering isopleths for the Si content of the mylonitic K-white mica (3.06–3.19 apfu) and the *P–T* fields of biotite-absent and garnet-absent mylonitic assemblages. Corresponding intersections occur at <475°C and <7 kbar in the calculated paragenetic fields of chlorite+K-white mica+paragonite+plagioclase+rutile+titanite+ilmenite (Figure 5).

6.3 | Modelling results for amphibolite CER4

A pseudosection was calculated for the bulk-rock composition of amphibolite CER4 to constrain the *P–T* conditions of the M_1 event (Figure 6). Calcic–sodic amphibole appears from 370°C at 2 kbar and 525°C at 15 kbar. From 525°C and 9 kbar towards higher temperature and pressure conditions two amphibole types (Na-amphibole and Ca-amphibole) coexist. Chlorite breaks down at 600°C, 2 kbar and 550°C, 15 kbar. Plagioclase occurs only below 7 (350°C)—13 kbar (600°C). Garnet is present over almost

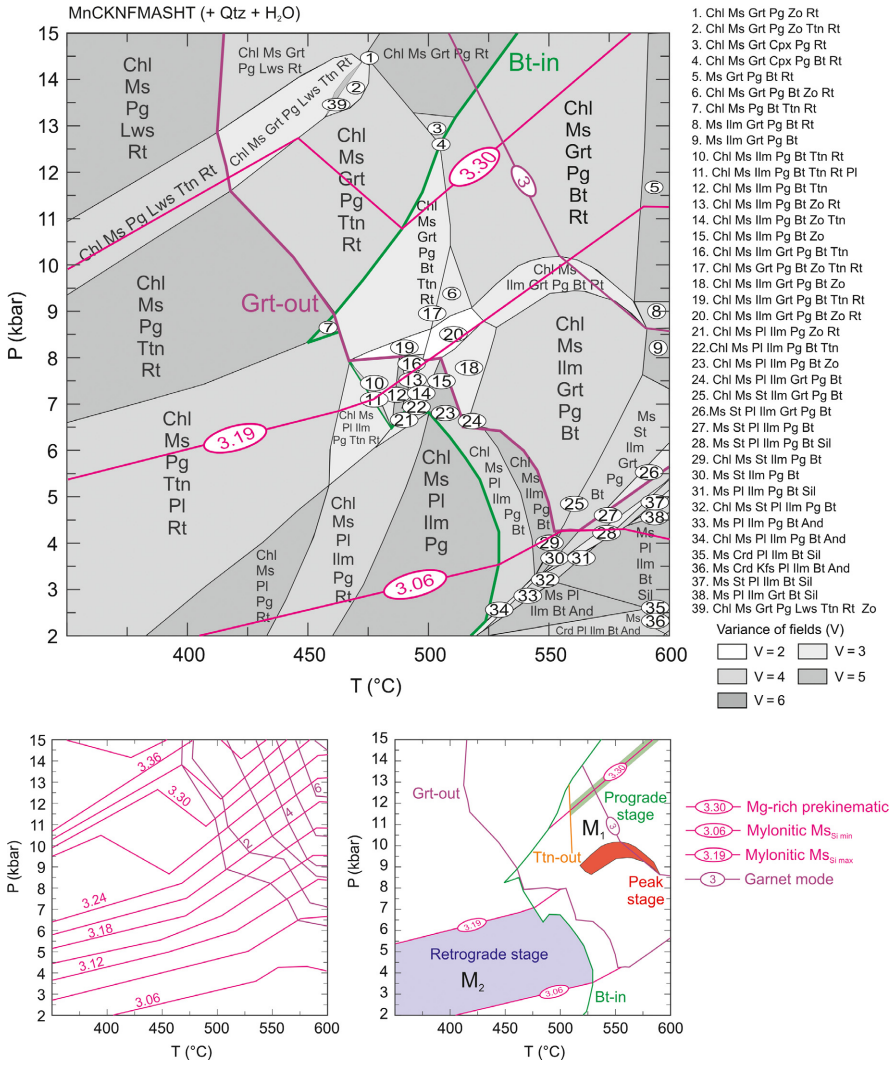

FIGURE 5 *P T* pseudosection for PC1 with K white mica isopleths (expressed in apfu), garnet isomodes (expressed in vol.%) and the selected constraints for the M_1 event (prograde and peak stages) and M_2 event (retrograde stage). The biotite in curve and the garnet out curve are marked. Mineral abbreviations are Ms (K white mica), Chl (chlorite), Pg (Na white mica), Grt (garnet), Bt (biotite), Pl (plagioclase), Kfs (K feldspar), Ilm (ilmenite), Rt (rutile), Ttn (titanite), Lws (lawsonite), Zo (zoisite), And (andalusite), Sil (sillimanite), St (staurolite), Crd (cordierite)

the entire *P–T* grid except below 4 kbar at 450–525°C and below 400°C. The ilmenite-in curve runs through 450°C–2 kbar and 530°C–15 kbar. Titanite is stable from 350 to 525°C. The calculated isopleths corresponding to the analysed garnet core composition intersects at 530°C and 5 kbar in the paragenetic field amphibole+plagioclase+garnet+chlorite+quartz+ilmenite in agreement with the observed M_1 paragenesis. The isopleths representing the garnet rim composition ($Alm_{58}Grs_{23}Sps_{11}Prp_5$; Molli et al., 2002) intersect at 550°C and 6 kbar (Figure 6), defining the peak stage of the M_1 event.

The pseudosection calculated for the fractionated bulk-composition (see above) constrains the M_2 conditions (Figure 7). The garnet stability field in the *P–T* pseudosection occurs above 475°C at 15 kbar and 595°C at 2 kbar. The Ca-amphibole-in curve is located at 350°C–6 kbar and 525°C–15 kbar. Towards higher temperatures and lower pressures, Ca-amphibole replaces clinopyroxene. Two coexisting amphibole types (Ca-amphibole and Na-amphibole) are present at high temperatures and high pressures. Chlorite disappears above 525°C at 10 kbar. Plagioclase breaks down above 7 (350°C)–13 (600°C) kbar. Ilmenite occurs above 450°C, 2 kbar and 550°C, 15 kbar. Titanite appears only in the 350–525°C range. Zoisite is present below 550°C (clinozoisite at <370°C) and is here assumed to be equivalent to epidote in the Fe^{3+}-free system. The calculated paragenesis corresponding to the observed M_2 (amphibole, plagioclase, epidote, chlorite, titanite, quartz) occurs at 425–525°C and 3–10 kbar (Figure 8). The minimum anorthite component in Pl_2 (molar fraction of An = 0.2) constrains the maximum pressure of M_2 at 8 kbar.

7 | DISCUSSION

7.1 | *P–T–D* path of the mylonites from the Variscan basement at Cerreto pass

Mylonites from shear zones, albeit forming a limited portion of rock outcrops, are first-order features for understanding plate tectonics (Bercovici & Ricard, 2012). Because of the localization of intense strain, mylonites are considered to have the potential to record metamorphic

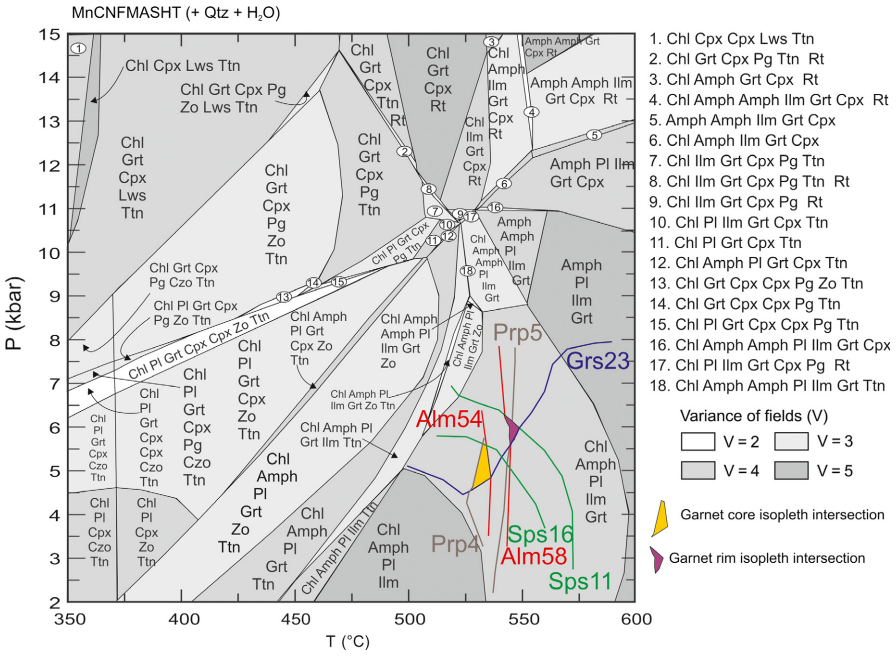

FIGURE 6 *P T* pseudosection for amphibolite CER4. The M_1 stage is constrained by garnet isopleths. Mineral abbreviations are as in Figure 5, with the addition of Amph (amphibole), Cpx (clinopyroxene), Czo (clinozoisite)

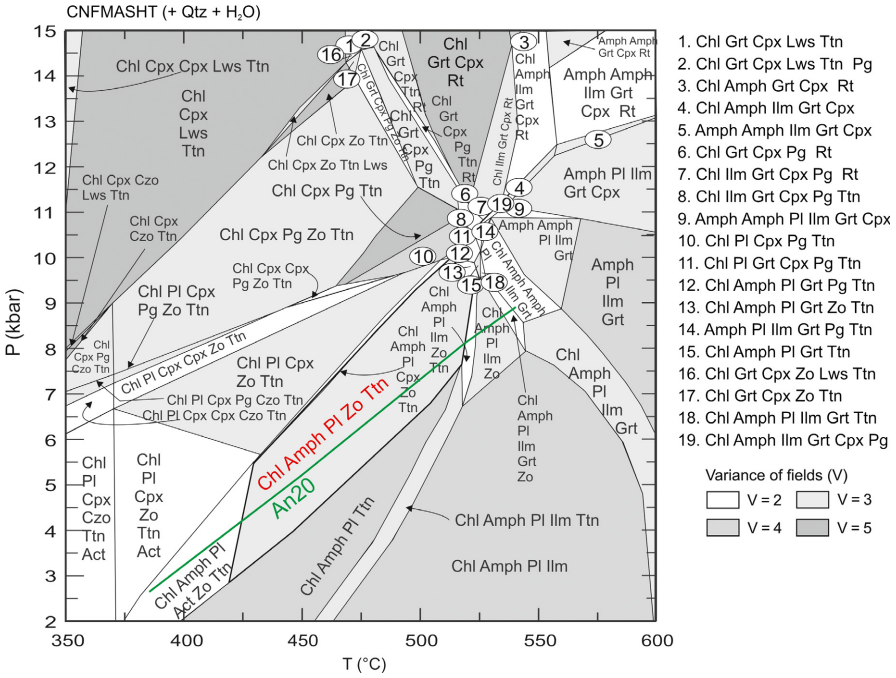

FIGURE 7 *P T* pseudosection for the M_2 stage in amphibolite CER4. The red coloured paragenesis corresponds to the observed one. Mineral abbreviations are as in Figures 5 and 6. The isopleth related to the maximum anorthite content in Pl_2 is shown

conditions of syn- to post-shearing (i.e. retrogression) events (Cirrincione, Fazio, Ortolano, Pezzino, & Punturo, 2012). Associated studies on adjacent less deformed/undeformed portions of wall rocks may provide hints on the pre-shearing metamorphic history. Our study indicates that extended portions of *P–T* paths, including pre-shearing stages, can be reconstructed even from mylonites by combining microstructural analysis, mineral-chemistry and thermodynamic modelling. In favourable circumstances, such as the Cerreto Pass mylonites, metamorphic conditions predating and during the mylonitic event are constrained from a small volume of rock at thin-section scale. In our case study, a clockwise *P–T–D* path for micaschist PC1 belonging to the Variscan basement at the Cerreto pass was reconstructed. This path includes two metamorphic events (M_1 and M_2; Figure 8). In particular, the M_1 event consists of (1) a high-*P* prograde stage (*P–T* conditions above 11 kbar and 510°C) recognized by Mg-rich cores in deformed K-white mica grains and a biotite-bearing, titanite-free paragenesis; (2) a peak temperature stage (550–590°C at 9–10 kbar), during which the M_1 paragenesis equilibrated. Ilmenite, which is not present in the

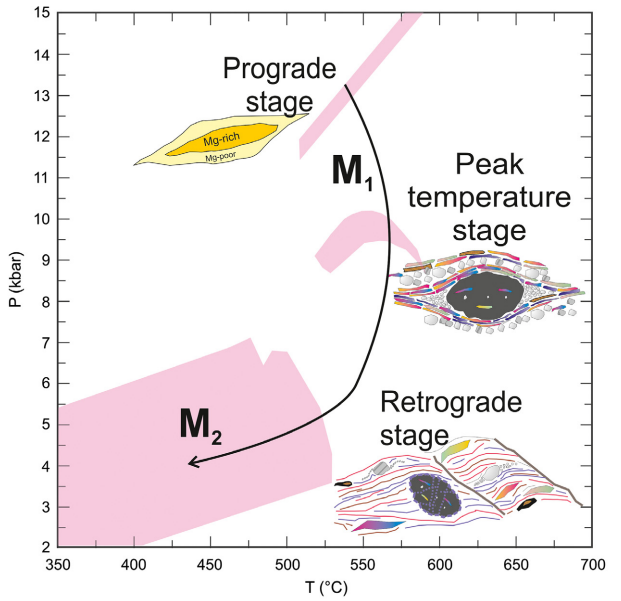

EVENT	STAGE	MICROSTRUCTURES	CONSTRAINING PHASES	*P-T* ESTIMATES
M_1	PROGRADE	Mica-fish cores	- Mg-rich prekinematic K-white mica (Si = 3.30) - Biotite-bearing titanite-free parageneses	> 510 °C > 11 kbar
M_1	PEAK	Garnet porphyroclasts	- Garnet-bearing paragenesis - Garnet pseudomorph mode (3 vol. %)	= 550–590 °C = 9–10 kbar
M_2	RETROGRADE	Mylonitic fabric	- Mylonitic K-white mica (Si = 3.06–3.19) - Biotite-absent parageneses - Garnet-absent parageneses	< 475 °C < 7 kbar

FIGURE 8 *P T D* path for the Cerreto micaschists. The table contains a summary of the tectono metamorphic evolution, with the microstructures, the constraining phases and the corresponding *P T* estimates. The pink figures mark the *P T* constraints in the micaschist

paragenesis of the prograde stage, formed during the peak stage. The M_2 event occurred during the retrograde stage (below 475°C and 7 kbar) and is represented by K-white mica oriented along the mylonitic foliation and by the absence of garnet and biotite. During the M_2 event, a well-developed mylonitic fabric developed (mylonitic foliation, shear bands, asymmetric foliations boudins, quartz oblique foliation). Paragonite was predicted to be present during the metamorphic evolution of the micaschist, but it was not found in PC1 (Table 4). However, this mineral can be easily overlooked, e.g. because of a very small grain size. Indeed, high-magnification observations with a field emission scanning microscopy on another micaschist from the Cerreto pass (sample PC23) revealed the existence of fine-grained paragonite flakes (10–50 μm wide, only a few μm thick; Figure 2f) intergrown with K-white mica. The bulk composition of the paragonite-bearing micaschist PC23 is similar to the bulk composition of PC1. In particular, the $Na_2O/(Na_2O+K_2O)$ ratios in PC23 and PC1 are 0.35 and 0.37, respectively. Although high-magnification observations with a field emission scanning microscopy are not available for PC1, it is conceivable that very fine-grained paragonite may also be present in this sample, in agreement with the pseudosection calculation result. Another apparent discrepancy between the observed M_2 mineral assemblage in micaschist PC1 (K-white mica+chlorite+plagioclase+quartz+titanite) and the predicted paragenesis (K-white mica+chlorite+plagioclase+quartz+paragonite+titanite+rutile+ilmenite) is the presence of low amounts of ilmenite and rutile (calculated mode for ilmenite and rutile in the retrograde stage is below 1 vol.%; Table 4). Substitutions of Al and F for Ti and O in titanite should extend the *P–T* stability of the titanite solid-solution (Tropper, Manning, & Essene, 2002). However, the calculation presented in this work considers titanite only as a pure ideal phase, with consequences on the titanite stability and its relationships with Ti-bearing minerals.

During the M_1 event, the amphibolite associated with the micaschist records a prograde stage at 530°C and 5 kbar, followed by peak temperature conditions at 550°C at 6 kbar (Figure 6). The retrograde paragenesis amphibole+plagioclase+epidote+chlorite+titanite+quartz developed at 425–525°C and 3–8 kbar (M_2). Although no extended *P–T* path could be reconstructed for the amphibolite, the obtained *P–T* conditions for amphibolite CER4 are quite different from those of the micaschist for the M_1 event but compatible for the M_2 event. Thus, the results from the thermodynamic modelling suggest a common retrograde evolution for the two rock types.

The obtained *P–T–D* path (Figure 8) points to a single metamorphic loop experienced by the Cerreto micaschist and amphibolite during the Variscan orogeny. The initial

TABLE 4 Observed and calculated paragenesis in micaschist PC1 and in amphibolite CER4 related to different metamorphic events. See text for the microstructural position of each mineral

	PC1	CER4
M_1		
Observed	Grt+Ms+Bt+Chl+Qtz+Rt+Ilm	Grt+Amph+Pl+Qtz+Ilm+Chl
Calculated	Grt+Ms+Bt+Chl+Qtz+Rt+Ilm+Pg	Grt+Amph+Pl+Qtz+Ilm+Chl
M_2		
Observed	Ms+Chl+Pl+Qtz+Ttn	Amph+Pl+Chl+Qtz+Ep+Ttn
Calculated	Ms+Chl+Pl+Qtz+Pg+Ttn+Rt+Ilm	Amph+Pl+Chl+Qtz+Ep+Ttn

prograde high-*P* stage (>11 kbar and >510°C) testifies a burial to 40 km and more during collision-related thickening of the crust. Peak temperatures of 550–590°C at 9–10 kbar followed the peak pressure. This suggests that heating by thermal equilibration occurred after the exhumation had already begun (see England & Thompson, 1984). Similar *P–T* paths have been reported from other collisional zones worldwide (e.g., Fiannacca, Lo Pò, Ortolano, Cirrincione, & Pezzino, 2012; Massonne, 2016; Massonne & Calderón, 2008; Massonne & Toulkeridis, 2012; Rötzler, Schumacher, Maresch, & Willner, 1998). The retrograde stage, accompanied by mylonitic deformation, is related to an exhumation process along ductile shear zones. Two tectonic scenarios can be proposed for the recognized retrograde stage in the Cerreto mylonites: (1) a post-Variscan intracontinental strike-slip shearing (Marroni, Molli, Montanini, & Tribuzio, 1998; Martini, Rau, & Tongiorgi, 1986; Massari, 1986; Matte, 2001; Padovano, Dörr, Elter, & Gerdes, 2014; Padovano, Elter, Pandeli, & Franceschelli, 2012; Ricci & Serri, 1975); (2) a Jurassic rifting stage that preludes the opening of the Western Tethys (Beltrando, Zibra, Montanini, & Tribuzio, 2013; Froitzheim & Manatschal, 1996; Mohn, Manatschal, Beltrando, Masini, & Kusznir, 2012; Mohn, Manatschal, Müntener, Beltrando,
& Masini, 2010; Molli et al., 2002; Montanini, Tribuzio, & Anczkiewicz, 2006).

7.2 | Implications for the pre-Alpine evolution of the Northern Apennine basement

Only three *P–T* paths have so far been presented for the pre-Alpine metamorphism in the Variscan basement of the Northern Apennines: Cerreto pass (Molli et al., 2002; and this work), Larderello (Bertini, Elter, & Talarico, 1994) 73 km SSE of the Cerreto pass, and Pontremoli (Lo Pò, Braga, Massonne, Molli, et al., 2016) 25 km WNW of the Cerreto pass.

Molli et al. (2002) investigated the metamorphic evolution of the micaschist complex at Cerreto pass, postulating an early metamorphic event at the garnet-amphibolite or eclogite facies, but did not constrain the pre-peak stage by geothermobarometry. These authors used classical thermobarometry to constrain the peak conditions at 650°C and 8 kbar for the amphibolites and 630°C and 8.5 kbar for the micaschists. These *P–T* conditions are ~50°C higher and 1 kbar lower than those calculated in this study for micaschist PC1. Considering 2σ-errors in the range of 5% for the temperature estimate and 10% in the pressure value (Massonne, 2013) determined through thermodynamic modelling, the previous *P–T* constraints overlap with the thermobaric constraints derived in this study. As micaschist and amphibolite are deformed together and show the same structural features (e.g. pre-kinematic relicts and mylonitic fabric), we infer that they shared a common metamorphic evolution from at least peak temperature conditions onward. The $^{40}Ar/^{39}Ar$ age determined for the amphibolites (328–312 Ma, Molli et al., 2002) record cooling below ≈500°C. These ages therefore constrain the inception of the retrograde evolution in the micaschists which occurred at <475°C and <7 kbar (this study).

Bertini et al. (1994) reconstructed the pre-Alpine *P–T* history of the gneiss complex in the Larderello subsurface through classical geothermobarometry and the stability fields of staurolite, muscovite, andalusite and cordierite. These authors estimated peak conditions of 500–600°C and 7 kbar, followed by an isothermal decompression to 2–3.5 kbar at 500–600°C, for the pre-Alpine history. Bertini et al. (1994) interpreted the obtained *P–T* path as related to a fast tectonic exhumation after the Variscan collision. The isothermal decompression stage, invoked by these authors, is different from the retrograde branch (from the peak temperature stage to the retrograde stage) of our *P–T–D* path that proposes a concomitant diminution of pressure with decreasing temperature. The contrasting retrograde evolution of the two complexes (Figure 9) suggests that they were related to different sectors or units of the former Variscan belt.

The Pontremoli garnet-bearing micaschist underwent a metamorphic evolution characterized by a prograde path starting at 530°C and 5.5 kbar, a metamorphic peak temperature of 575°C at 7 kbar (in early Permian times: 293 Ma), subsequent peak pressure of 8 kbar at 520°C and a retrogression at 475–520°C and 2–7 kbar (Lo Pò, Braga, Massonne, Molli, et al., 2016). The peak conditions of the Cerreto metamorphic rocks (328–312 Ma) were reached earlier and at different pressures (9–10 *v.* 7 kbar in the Pontremoli basement; Figure 9). Hence, we propose that Cerreto and Pontremoli basement rocks also belong to distinct tectonic units or sectors of the former South Variscan belt, according to the present day Apenninic tectonic setting which supports their attribution to different crustal segments (i.e. Apenninic palaeotectonic domains; Molli, 2008).

7.3 | Comparison between the Cerreto and neighbouring south-European Variscan units

The metamorphic evolution of the Cerreto micaschists resembles the Variscan history of chloritoid schists from the Inner Zone of the Variscan chain of nearby NE Sardinia (Cruciani, Franceschelli, Massonne, Carosi, & Montomoli, 2013). Through the same thermodynamic approach (pseudosections+isopleths of Si content in K-white mica) used in this work, Cruciani et al. (2013) constrained a high-*P* stage (18 kbar at 460–500°C) before a Barrovian-type metamorphism, the peak temperature of which is 540–

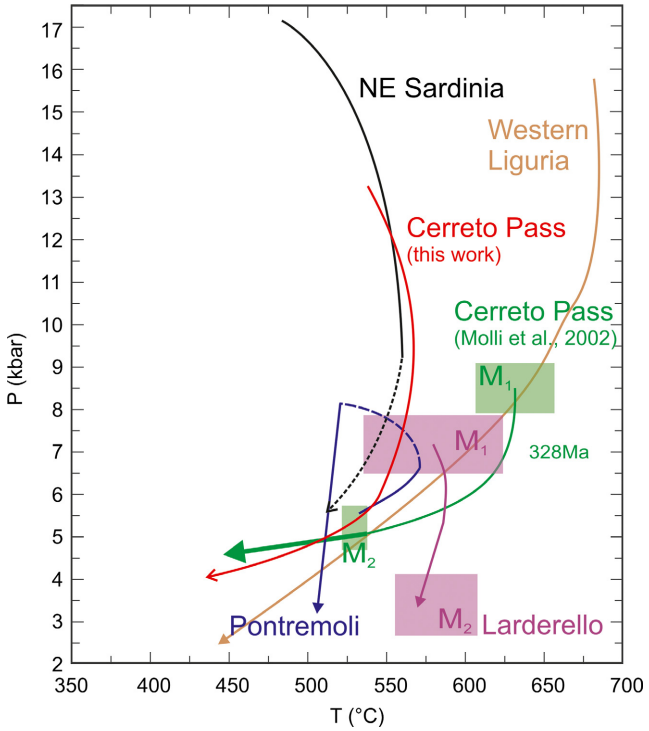

FIGURE 9 The Cerreto *P T* path (red arrow) compared with the thermobaric trajectories proposed for some Variscan segments in the Northern Apennines, Sardinia and Liguria: violet arrows and boxes for the Larderello gneiss complex (Northern Apennines; Bertini et al., 1994); green arrows and boxes for the Cerreto amphibolites (Northern Apennines; Molli et al., 2002); light blue arrow for the Pontremoli micaschist (Northern Apennines; Lo Pò, Braga, Massonne, Molli, et al., 2016); black continuous to dashed arrow for the Inner Zone of the Sardinian basement (Cruciani et al., 2013); brown arrow for the eclogites from Savona Crystalline Massif of the Ligurian Alps (Giacomini et al., 2007 and references therein)

570°C at 7–10 kbar. The *P–T* estimates and the overall clockwise shape of the *P–T* path obtained for the Cerreto rocks (*HP* prograde stage at >11 kbar and >510°C and peak temperature of 550–590°C at 9–10 kbar) are similar to the Sardinian thermobaric trajectory (Cruciani et al., 2013). Both basements also share decreasing pressure conditions during Barrovian metamorphism and diachronous pressure and temperature peaks, distinctive of orogenic belts affected by crustal thickening and exhumation (Cruciani et al., 2013; England & Thompson, 1984). The Variscan basement in the Northern Apennines and NE Sardinia share some other similarities, namely the E-MORB affinity of the amphibolites and the cooling $^{40}Ar/^{39}Ar$ ages (Carmignani et al., 1994; Molli et al., 2002). Indeed, the Variscan basement of the Inner Zone in Sardinia experienced a transpressive shearing tectonism that developed, for instance, along the Posada-Asinara Line at 325–315 Ma (Carosi, Montomoli, Tiepolo, & Frassi, 2012; Di Vincenzo, Carosi, & Palmeri, 2004; Elter & Pandeli, 2005). This age is consistent with the age determination of 328–312 Ma in the amphibolites from the Cerreto pass, interpreted to record regional metamorphic cooling below ~500°C (Molli et al., 2002). Another analogy is the protolith nature for the metapelitic rocks. According to the Fe_2O_3/K_2O *v.* SiO_2/Al_2O_3 diagram by Herron (1988), the chloritoid schists from NE Sardinia developed from immature clastic sediments similarly to the micaschists from the Cerreto pass. Furthermore, both are characterized by Ca-poor bulk rock compositions. Hence, it is conceivable that the metamorphic rocks studied here and from NE Sardinia represent the same geotectonic collisional zone, as suggested by Molli et al. (2002).

In the Inner Zone of the Variscan chain in Sardinia, eclogites enclosed in medium grade metapelites also record a high-*P* stage at 13–15 kbar and 610–700°C (Cortesogno, Gaggero, Oggiano, & Paquette, 2004; Cruciani, Montomoli, Carosi, Franceschelli, & Puxeddu, 2015). Both eclogites and metapelites re-equilibrated under amphibolite-facies conditions during the Variscan collision at 320–315 Ma (Di Vincenzo et al., 2004). The Sardinian medium-grade metapelites and eclogites were correlated with the eclogite-bearing Gneiss-Amphibolite Complex of the Ligurian Alps (Cortesogno et al., 2004). In the Gneiss-Amphibolite Complex, the high-*P* metamorphic overprint of the eclogite relicts occurred at 392–376 Ma, and was followed by an amphibolite facies re-equilibration at 333 ± 7 Ma (Giacomini, Braga, Tiepolo, & Tribuzio, 2007; Figure 9). Although eclogitic relicts have not been found in the Cerreto basement, the comparable metamorphic evolution of metapelites from the Cerreto Pass, NE Sardinia and Ligurian Alps (high-*P* stage followed by an amphibolite facies overprint) supports the palaeotectonic correlation between the Cerreto basement, the Inner Zone of the Sardinia Variscan belt and the Gneiss-Amphibolite Complex of the Ligurian Alps.

8 | CONCLUSIONS

When pre-kinematic and syn-kinematic minerals occur in the same mylonitic rock, the application of thermodynamic modelling has the potential to reveal the thermobaric conditions occurred before and during the high-strain event that obliterates most of earlier metamorphic stages. The reconstruction of complete polyphase *P–T* evolutions of mylonites is useful to unravel the tectono-metamorphic history of crystalline basements now dismembered in different domains of orogenic belts.

Micaschists and amphibolites from the Cerreto pass are remnants of the Variscan basement reworked within the Northern Apennine nappe stack. A clockwise *P–T–D* path (prograde, temperature peak and retrograde stages) has

been established from analysis of a mylonitic metapelite and amphibolite. A peak pressure in excess of 11 kbar has been determined in the micaschist, showing the first occurrence of a Variscan high-*P* event in the Northern Apennines. This event was caused by crustal thickening during the collision of Gondwana and Laurussia. The high-*P* stage was followed by metamorphism at peak temperature of 550–590°C at 9–10 kbar. The post-peak evolution occurred at 328–312 Ma in micaschist and adjacent amphibolite, which both experienced similar *P–T* conditions. The retrogression stage at <475°C, <7 kbar at the Cerreto pass, responsible for the well-developed mylonitic fabric, is most likely related to the exhumation of Variscan crust along ductile shear zones.

The Variscan basements at Larderello (gneiss complex) and Pontremoli show different metamorphic evolutions suggesting provenances from different units or sectors of the former Variscan belt. In contrast, metamorphic evolution and timing of the Cerreto Variscan basement is similar to those inferred for micaschists from NE Sardinia and Ligurian Alps. This new finding supports a palaeotectonic correlation of these Variscan basement areas.

ACKNOWLEDGEMENTS

We thank Professors G. Gasparotto and E. Dinelli from the University of Bologna who helped us in SEM observations and XRF analyses, respectively. We are also grateful to T. Theye (Universität Stuttgart) for assistance in the EMP analyses. The suggestions of L. Gaggero and three anonymous reviewers improved the manuscript. We also thank the editor D. Robinson for his comments and editorial handling. Funding from the University of Bologna (the Marco Polo programme to D.L.P. and RFO to R.B.) is acknowledged.

ORCID

Roberto Braga http://orcid.org/0000-0001-8210-6658

REFERENCES

Batini, F., Brogi, A., Lazzarotto, A., Liotta, D., & Pandeli, E. (2003). Geological features of Larderello Travale and Mt. Amiata geother mal areas (southern Tuscany, Italy). *Episodes*, *26*, 239 244. Beltrando, M., Zibra, I., Montanini, A., & Tribuzio, R. (2013). Crustal thinning and exhumation along a fossil magma poor distal margin preserved in Corsica: A hot rift to drift transition? *Lithos*, *168*, 99 112.

Bercovici, D., & Ricard, Y. (2012). Mechanisms for the generation of plate tectonics by two phase grain damage and pinning. *Physics of the Earth and Planetary Interiors*, *202 203*, 27 55.

Bernhardt, H. J., Massonne, H. J., Reinecke, T., Reinhardt, J., & Willner, A. (1995). Digital element distribution maps, an aid for petrological investigations. *Berichte der Deutschen Mineralogischen Gesellschaft, Beihefte zum European Journal of Mineralogy*, *7*, 28.

Bernoulli, D. (2001). Mesozoic Tertiary carbonate platforms, slopes and basins of the external Apennines and Sicily. In F. Vai & I. P. Martini (Eds.), *Anatomy of an orogen: The Apennines and adjacent mediterranean basins* (pp. 307 325). The Netherlands: Springer.

Bertini, G., Casini, M., Gianelli, G., & Pandeli, E. (2006). Geological structure of a long living geothermal system, Larderello, Italy. *Terra Nova*, *18*, 163 169.

Bertini, G., Elter, F. M., & Talarico, F. (1994). Evidenze di una fase estensionale pre triassica nel complesso degli gneiss nell'area geotermica di Larderello (Toscana meridionale). *Studi Geologici Camerti, Volume speciale*, *1*, 129 137.

Braga, R., & Cinelli, G. (2014). The gabbro and serpentinized peri dotite of Bonassola (Bracco Levanto ophiolite, Italy) An extre mely low natural radiation area to improve in situ gamma spectrometry. *Ofioliti*, *39*, 43 49.

Brandelik, A. (2009). CALCMIN An EXCEL™ Visual Basic applica tion for calculating mineral structural formulae from electron micro probe analyses. *Computers and Geosciences*, *35*, 1540 1551.

Carmignani, L., Carosi, R., Di Pisa, A., Gattiglio, M., Musumeci, G., Oggiano, G., & Pertusati, P. C. (1994). The Hercynian chain in Sardinia (Italy). *Geodinamica Acta*, *7*, 31 47.

Carosi, R., Montomoli, C., Tiepolo, M., & Frassi, C. (2012). Geochronological constraints on post collisional shear zones in the Variscides of Sardinia (Italy). *Terra Nova*, *24*, 42 51.

Cirrincione, R., Fazio, E., Ortolano, G., Pezzino, A., & Punturo, R. (2012). Fault related rocks: Deciphering the structural metamor phic evolution of an accretionary wedge in a collisional belt, NE Sicily. *International Geology Review*, *54*, 940 956.

Connolly, J. A. D. (1990). Multivariable phase diagrams: An algo rithm based on generalized thermodynamics. *American Journal of Science*, *290*, 666 718.

Connolly, J. A. D., & Petrini, K. (2002). An automated strategy for calculation of phase diagram sections and retrieval of rock proper ties as a function of physical conditions. *Journal of Metamorphic Geology*, *20*, 697 708.

Conti, P., Di Pisa, A., Gattiglio, M., & Meccheri, M. (1993). The Pre Alpine Basement in the Alpi Apuane (Northern Apennines, Italy). In J. F. Von Raumer, & F. Neubauer (Eds.), *Pre Mesozoic geology in the Alps* (pp. 609 621). Heidelberg: Springer Verlag.

Cortesogno, L., Gaggero, L., Oggiano, G., & Paquette, J. L. (2004). Different tectono thermal evolutionary paths in eclogitic rocks from the axial zone of the Variscan chain in Sardinia (Italy) com pared with the Ligurian Alps. *Ofioliti*, *29*, 125 144.

Cruciani, G., Franceschelli, M., Massonne, H. J., Carosi, R., & Mon tomoli, C. (2013). Pressure temperature and deformational evolu tion of high pressure metapelites from Variscan NE Sardinia, Italy. *Lithos*, *175 176*, 272 284.

Cruciani, G., Montomoli, C., Carosi, R., Franceschelli, M., & Pux eddu, M. (2015). Continental collision from two perspectives: A review of Variscan metamorphism and deformation in northern Sardinia. *Periodico di Mineralogia*, *84*, 1 44.

Di Vincenzo, G., Carosi, R., & Palmeri, R. (2004). The relationship between tectono metamorphic evolution and argon isotope records in white mica: Constraints from in situ ^{40}Ar ^{39}Ar laser analysis of the Variscan basement of Sardinia. *Journal of Petrology*, *45*, 1013 1043.

Elter, P. (1975). L'ensemble ligure. *Bulletin de la Sociéte Géologique de France*, *17*, 984 997.

Elter, F. M., & Pandeli, E. (2005). Structural metamorphic correlations between three Variscan segments in southern Europe: Maures Mas sif (France), Corsica (France) Sardinia (Italy) and Northern Appen nines (Italy). *Journal of Virtual Explorer*, *19*, 1 19.

England, P. C., & Thompson, A. B. (1984). Pressure temperature time paths of regional metamorphism I. Heat transfer during the evolu tion of regions of thickened continental crust. *Journal of Petrol ogy*, *25*, 894 928.

Fiannacca, P., Lo Pò, D., Ortolano, G., Cirrincione, R., & Pezzino, A. (2012). Thermodynamic modeling assisted by multivariate statistical image analysis as a tool for unraveling metamorphic P T d evolution: An example from ilmenite garnet bearing metapelite of the Peloritani Mountains, Southern Italy. *Mineralogy and Petrology*, *106*, 151 171.

Franceschelli, M., Gianelli, G., Pandeli, E., & Puxeddu, M. (2004). Variscan and Alpine metamorphic events in the northern Apenni nes (Italy): A review. *Periodico di Mineralogia*, *73*, 43 56.

Froitzheim, N., & Manatschal, G. (1996). Kinematics of Jurassic rift ing, mantle exhumation, and passive margin formation in the Aus troalpine and Penninic nappes (eastern Switzerland). *Geological Society of America Bulletin*, *108*, 1120 1133.

Fuhrman, M. L., & Lindsley, D. H. (1988). Ternary feldspar model ing and thermometry. *American Mineralogist*, *73*, 201 215.

Giacomini, F., Braga, R., Tiepolo, M., & Tribuzio, R. (2007). New con straints on the origin and age of Variscan eclogitic rocks (Ligurian Alps, Italy). *Contributions to Mineralogy and Petrology*, *153*, 29 53.

Herron, M. M. (1988). Geochemical classification of terrigenous sands and shales from core and log data. *Journal of Sedimentary Petrology*, *58*, 820 829.

Holland, T., Baker, J., & Powell, R. (1998). Mixing properties and activ ity composition relationships of chlorites in the system MgO FeO Al_2O_3 SiO_2 H_2O. *European Journal of Mineralogy*, *10*, 395 406.

Holland, T. J. B., & Powell, R. (1991). A compensated Redlich Kwong (CORK) equation for volumes and fugacities of CO_2 and H_2O in the range 1 bar to 50 kbar and 100 1600°C. *Contribu tions to Mineralogy and Petrology*, *109*, 265 273.

Holland, T. J. B., & Powell, R. (1996). Thermodynamics of order dis order in minerals: II. Symmetric formalism applied to solid solu tions. *American Mineralogist*, *81*, 1425 1437.

Holland, T. J. B., & Powell, R. (1998). An internally consistent ther modynamic data set for phases of petrological interest. *Journal of Metamorphic Geology*, *16*, 309 343.

Leake, B. E., Woolley, A. R., Birch, W. D., Burke, E. A. J., Ferraris, G., Grice, J. D., . . . Whittaker E. W. (2004). Nomenclature of amphiboles: Additions and revisions to the International Mineralogical Associa tions amphibole nomenclature. *American Mineralogist*, *89*, 883 887.

Lo Pò, D., & Braga, R. (2014). Influence of ferric iron on phase equi libria in greenschist facies assemblages: The hematite rich metasedimentary rocks from the Monti Pisani (Northern Apenni nes). *Journal of Metamorphic Geology*, *32*, 371 387.

Lo Pò, D., Braga, R., & Massonne, H. J. (2016). Petrographic, min eral and pressure temperature constraints on phyllites from the Variscan basement at Punta Bianca, Northern Apennines, Italy. *Italian Journal of Geosciences*, *135*, 489 502.

Lo Pò, D., Braga, R., Massonne, H. J., Molli, G., Montanini, A., & Theye, T. (2016). Fluid induced breakdown of monazite in medium grade metasedimentary rocks of the Pontremoli basement (Northern Apennines, Italy). *Journal of Metamorphic Geology*, *34*, 63 84.

Marroni, M., Molli, G., Montanini, A., & Tribuzio, R. (1998). The association of continental crust rocks with ophiolites in the Northern Apennines (Italy): Implications for the continent ocean transition in the Western Tethys. *Tectonophysics*, *292*, 43 66.

Martini, I. P., Rau, A., & Tongiorgi, M. (1986). Syntectonic sedimen tation in a Middle Triassic rift, northern Apennines, Italy. *Sedi mentary Geology*, *47*, 191 219.

Massari, F. (1986). Some thoughts on the Permo Triassic evolution of the South Alpine area (Italy). *Memorie della Società Geologica Italiana*, *34*, 179 188.

Massonne, H. J. (2010). Phase relations and dehydration behaviour of calcareous sediments at very low to low grade metamorphic con ditions. *Periodico di Mineralogia*, *79*, 21 43.

Massonne, H. J. (2012). Formation of amphibole and clinozoisite epi dote in eclogite owing to fluid infiltration during exhumation in a subduction channel. *Journal of Petrology*, *53*, 1969 1998.

Massonne, H. J. (2013). Constructing the pressure Temperature path of ultrahigh pressure rocks. *Elements*, *9*, 267 272.

Massonne, H. J. (2016). Tertiary high pressure metamorphism recorded in andalusite bearing mica schist, southern Pirin Mts, SW Bulgaria. *European Journal of Mineralogy*, *28*, 1187 1202.

Massonne, H. J., & Calderón, M. (2008). P T evolution of metapelites from the Guarguaráz Complex, Argentina Evidence for Devo nian crustal thickening close to the western Gondwana margin. *Revista Geológica de Chile*, *35*, 215 231.

Massonne, H. J., & Toulkeridis, T. (2012). Widespread relics of high pressure metamorphism confirm major terrane accretion in Ecua dor: A new example from the Northern Andes. *International Geology Review*, *54*, 67 80.

Massonne, H. J., & Willner, A. P. (2008). Phase relations and dehy dration behaviour of psammopelite and mid ocean ridge basalt at very low grade to low grade metamorphic conditions. *European Journal of Mineralogy*, *20*, 867 879.

Matte, P. (2001). The Variscan collage and orogeny (480 290 Ma) and the tectonic definition of the Armorica microplate: A review. *Terra Nova*, *13*, 122 128.

McLennan, S. M. (2001). Relationships between the trace element composition of sedimentary rocks and upper continental crust. *Geochemistry, Geophysics, Geosystems*, *2*, 1 24.

Mohn, G., Manatschal, G., Beltrando, M., Masini, E., & Kusznir, N. (2012). Necking of continental crust in magma poor rifted mar gins: Evidence from the fossil Alpine Tethys margins. *Tectonics*, *31*(1), TC1012.

Mohn, G., Manatschal, G., Müntener, O., Beltrando, M., & Masini, E. (2010). Unravelling the interaction between tectonic and sed imentary processes during lithospheric thinning in the Alpine Tethys margins. *International Journal of Earth Sciences*, *99*, 75 101.

Moine, B., & De La Roche, H. (1968). Nouvelle approche du problème de l'origine des amphibolites à partir de leur composi tion chimique. *Comptes Rendus de l'Académie des Sciences de Paris*, *267*, 2084 2087.

Molli, G. (2008). Northern Apennine Corsica orogenic system: An updated overview. *Geological Society, London, Special Publica tions*, *298*, 413 442.

Molli, G., Montanini, A., & Frank, W. (2002). MORB derived Varisican amphibolites in the Northern Apennine Basement: The Cerreto meta morphic slices (Tuscan Emilian Apennine, NW Italy). *Ofioliti*, *27*, 17 30.

Montanini, A., Tribuzio, R., & Anczkiewicz, R. (2006). Exhumation history of a garnet pyroxenite bearing mantle section from a

continent ocean transition (Northern Apennine ophiolites, Italy). *Journal of Petrology*, *47*, 1943 1971.

Padovano, M., Dörr, W., Elter, F. M., & Gerdes, A. (2014). The East Variscan Shear Zone: Geochronological constraints from the Capo Ferro area (NE Sardinia, Italy). *Lithos*, *196 197*, 27 41.

Padovano, M., Elter, F. M., Pandeli, E., & Franceschelli, M. (2012). The East Variscan Shear Zone: New insights into its role in the Late Carboniferous collision in southern Europe. *International Geology Review*, *54*, 957 970.

Pandeli, E., Gianelli, G., & Morelli, M. (2005). The crystalline units of the middle upper crust of the Larderello geothermal region (southern Tuscany, Italy): New data for their classification and tectono metamorphic evolution. *Bollettino Società Geologica Ital iana, Volume Speciale*, *3*, 139 155.

Powell, R., & Holland, T. J. B. (1999). Relating formulations of the thermodynamics of mineral solid solutions: Activity model ing of pyroxenes, amphiboles, and micas. *American Mineralo gist*, *84*, 1 14.

Ricci, C. A. (1968). Le rocce metamorfiche di natura basica e ultraba sica nelle serie a facies toscana. Studio chimico e petrografico. *Atti della Società Toscana di Scienze Naturali*, *75*, 1 67.

Ricci, C. A., & Serri, G. (1975). Evidenza geochimica sulla diversa affinità petrogenetica delle rocce basiche comprese nella serie a facies toscana. *Bollettino Società Geologica Italiana*, *94*, 1187 1198.

Rötzler, K., Schumacher, R., Maresch, W. V., & Willner, A. P. (1998). Characterization and geodynamic implications of contrast ing metamorphic evolution in juxtaposed high pressure units of the Western Erzgebirge (Saxony, Germany). *European Journal of Mineralogy*, *10*, 261 280.

Stüwe, K. (1997). Effective bulk composition change due to cooling: A model predicting complexities in retrograde reaction textures. *Contributions to Mineralogy and Petrology*, *129*, 43 52.

Taylor, S. R., & McLennan, S. M. (1985). *The continental crust: Its composition and evolution* (p. 312). Oxford: Blackwell Scientific.

Tropper, P., Manning, C. E., & Essene, E. J. (2002). The substitution of Al and F in titanite at high pressure and temperature: Experi mental constraints on phase relations and solid solution properties. *Journal of Petrology*, *43*, 1787 1814.

Vai, G. B. (2003). Development of the palaeogeography of Pangaea from Late Carboniferous to Early Permian. *Palaeogeography, Palaeoclimatology, Palaeoecology*, *196*, 125 155.

Vai, F., & Martini, I. P. (2001). *Anatomy of an orogen: The Apenni nes and adjacent mediterranean basins* (pp. 307 325). Springer, Netherlands: Kluwer Academic Publishers.

White, R. W., Powell, R., Holland, T. J. B., & Worley, B. A. (2000). The effect of TiO_2 and Fe_2O_3 on metapelitic assemblages at greenschist and amphibolite facies conditions: Mineral equilibria calculations in the system K_2O FeO MgO Al_2O_3 SiO_2 H_2O TiO_2 Fe_2O_3. *Journal of Metamorphic Geology*, *18*, 497 512.